Preprint
UCRL-JC-149930

Low-Dispersion Optical Fiber Highly Transparent in the UV Spectral Range

G.M. Ermolaeva, M.A. Eron'yan, K.V. Dukel'skii, A.V. Komarov, Yu.N. Kondratev, M.M. Serkov, M.N. Tolstoy, V.B. Shilov, V.S. Shevandin, H.T. Powell, and C.E. Thompson

This article was submitted to International Optical Congress "Optics – XXI century", Saint Petersburg, Russia, Oct 14-18, 2002

U.S. Department of Energy

Lawrence Livermore National Laboratory

October 1, 2002

Low-Dispersion Optical Fiber
Highly Transparent in the UV Spectral Range

G.M.Ermolaeva, M.A.Eron'yan, K.V.Dukel'skii, A.V.Komarov,
Yu.N.Kondratev, M.M.Serkov, M.N.Tolstoy, V.B.Shilov, and V.S.Shevandin.
Vavilov State Optical Institute, Saint-Petersburg, Russia

and

H. T. Powell, C. E. Thompson
Lawrence Livermore National Laboratory, Livermore, USA

Introduction

The fiber transport of sub-nanosecond laser pulses in the ultraviolet spectral region over significant distances, such as those found in the National Ignition Facility, requires special fibers. The National Ignition Facility (NIF) is a 192 arm, Nd-doped, phosphate glass laser that is being built for the U.S. Department of Energy by and at the Lawrence Livermore National Laboratory (LLNL). This facility will be used for Inertial Confinement Fusion (ICF) research. The ultraviolet (UV) light used for target irradiation is generated at the entrance to the target chamber by converting the fundamental laser wavelength to the third harmonic (351 nm).

The NIF Laser Diagnostic System's power diagnostic measures the UV laser power produced by each of the 192 arms. In this system, the diagnostic samples the laser pulse at the target chamber and a fiber transports this signal to detection and recording instrumentation located outside the target room. Pulses from four arms are delayed and multiplexed into a vacuum photodiode detector; a high bandwidth transient digitizer records the data. This basic structure is duplicated many times within the power diagnostic system.

System and measurement criteria, as well as NIF architecture, dictate the performance of these special fibers. A low temporal dispersion (i.e., high bandwidth), graded-index type fiber is required because step-index fibers do not possess the required bandwidth and single-mode fibers limit signal intensity. Physical path lengths (~60 meters) and diagnostic system measurement rise-time requirements determine allowable fiber attenuation and temporal dispersion. A large core diameter provides many propagation modes that, when averaged by the detector, allow the fiber to meet the amplitude noise criteria (<=0.5%) set by

diagnostic system requirements. A companion component, a LLNL designed fiber launch assembly, launches light into all available fiber modes. In addition, this assembly makes light launching into the fiber insensitive to changes in laser alignment while simultaneously sampling all parts of the laser beam equally.

In summary, fibers used for NIF ultraviolet laser diagnostics must meet the following criteria and have had to be developed:

Fiber Characteristic	**Requirement**
Type	Graded-index
Temporal dispersion (@351 nm)	< 0.9 psec/m (goal: ≤ 0.5 psec/m)
Attenuation (@351 nm)	< 200 dB/km (goal: < 150 dB/km)
Numerical aperture (@351 nm)	0.13 ± 0.01
Core diameter	435 μm

Silica glass is a traditional optical medium with the greatest transparency in a wide spectral range. This fact can be illustrated by the wide use of silica glass in telecommunication, with the scale of manufacturing of the fibers lying in the range of tens or even hundreds of million of kilometers, which undoubtedly indicates advantages of silica glass over other optical materials (multicomponent optical glasses, vitreous chalcogenides, and zirconium-containing fluoride glasses, which were recently considered as possible alternatives for the vitreous silica [2]).

At the same time, the use of silica glass for the purposes of tele-communication is limited by three optical regions (windows of transparency), which, on the one hand, are determined by low optical losses related to scattering and absorption of impurity water, dissolved and bonded in the silica glass structure and, on the other, by the detectors of radiation available for these regions. These windows of transparency are 840 – 850, 1300 – 1310, and 1550 – 1650 nm. Feasibility of application of silica glass for transmitting optical signals in other spectral regions requires confirmation in the form of real measurements of the absorption coefficient in the fibers, including the regions of bands with low absorptance.

Transparency of silica-glass fibers in the UV spectral range

In the analysis of silica glass transparency in the UV spectral range, one has to pay attention to the fact that, methodologically, the main body of studies, along

these lines, was performed on relatively thin samples. This is why these studies allowed one to determine sufficiently well the fundamental absorption edge and positions of intense absorption bands with the absorption index "**a**" higher than 0.05 – 0.1 cm^{-1} [3]. In the units used for measuring the absorption in fibers, it corresponds to α=50,000–100,000 dB/km. In the visible range, silica glass is highly transparent ("**a**"< 0.01) [4]. The measurements of absorption in fibers made of pure silicon dioxide were performed by Khalilov et al. [5, 6]. The transparency region of silica glass is limited, from the short-wavelength side of fundamental absorption (158 nm), by the absorption associated with electronic transitions in the tetrahedrons [$SiO_{4/2}$], and from the long-wavelength side (2.86 mkm), by the vibrational transitions in the skeleton $[SiO_{4/2}]_\infty$ [7, 8]. In the industrial brands of silica glass, a complex absorption band is observed in the vicinity of 245 nm, consisting of two closely spaced bands (242 and 248 nm), associated with intrinsic defects of the glass, namely, with the oxygen vacancies [$O_{3/2}Si–SiO_{3/2}$] [9]. The reduction conditions of melting give rise to growth of this band. Some fibers manufactured from a synthetic glass by oxidation or hydrolysis of silicon tetrachloride show a band at 163 nm related to the intrinsic defects [$Si^{+}O_{3/2}$] [10].
The preforms from the glass obtained by oxidation or hydrolysis of silicon tetrachloride in the gaseous phase contain great amount of chlorine, which, being dissolved in the glass, interacts with the structure of the latter, which leads to appearance of the band at 330 nm [11].

At the same time, it is noteworthy that the drawing of the fiber, accompanied by breakage of the bond Si–O–Si, gives rise to appearance of the broad UV bands at 210 and 248 nm and the band 630 nm in the visible range [12, 13]. The drawing of the fiber, in some cases changes the ratio of the bands 210, 248, and 330 nm [13].

The efforts to obtain a highly transparent fiber should take into account the fact that the color centers may arise in the glass at the stage of manufacturing of preform and in the fiber at the stage of the preform drawing.

The light attenuation due to the Rayleigh scattering

Another factor that increases the light losses in the fibers is the light scattering. The light is scattered by any spatial inhomogeneities of the medium. In this paper, we do not take into account such specific types of the light scattering as the Brillouin and Raman scattering.

When analyzing the Rayleigh losses, as applied to the silica glass, one should take into account the scattering by fluctuations of density and concentration. The silica glass is virtually a single-component system. For this reason, only the density fluctuations may contribute to the Rayleigh scattering. The effect of the doping impurities providing the refractive index profile cannot be easily taken into account, but seems to be rather small due to smallness of their concentrations.

The relationship between the losses associated with the Rayleigh scattering, properties of the medium, and the light wavelength can be expressed in the form [14]:

$$\alpha_{Rs} = \frac{8\partial^3}{3ë^4}\left(n^8 p^2\right) \times kT_f \hat{a}_T, \qquad (1)$$

where, along with conventional constants, λ is the wavelength, n is the refractive index, p is the photoelastic constant of the glass, k is the Boltzmann constant, T_f is the vitrification temperature, and β_T is the isothermal compressibility.

According to [15], the absolute losses related to the Rayleigh scattering at 1.55 mkm are α_{Rs} = 0.18 dB/km. It is this small value that attracts attention of researchers to the range of 1.55 mkm. Extrapolation of spectral dependence of the losses to 350 nm yields 80 – 90 dB/km. This is the value that determines the lowest level of the losses which may be obtained in the fibers at this wavelength.

The refractive index profiles and dispersion characteristics

In the fibers employed for transmitting information, an important role is played by their dispersion properties, which are determined by three types of dispersion:

- material,
- intermode, and
- intramode.

When a laser with a spectral width of 0.2 nm is used as the light source, the material and intramode dispersions are negligibly small. The main factor that broadens the pulse in the multimode fibers is the intermode dispersion, which depends on the refractive index profile. The optimum function describing the refractive index profile (RIP) can be written in the form

$$n(r) = n_1 \sqrt{1 - 2\Delta_{rel}\left(\frac{r}{r_{core}}\right)^{\alpha_{profile}}}, \qquad (2)$$

where

$n(r)$ – is the radial refractive index,

n_1 – is the refractive index in the fiber core center,

$\Delta_{rel} = \frac{n_1 - n_2}{n_1}$ – is the relative increment of the refractive index controlling the fiber aperture,

n_2 – is the refractive index of the cladding.

r and r_{core} – are the current radius and radius of the core, and

$\alpha_{profile}$ – is the parameter of the profile in equation (2).

For $\alpha_{profile}$ =2, we obtain parabolic profile of the refractive index, while at $\alpha_{profile}=\infty$ the profile appears to be step-wise.

The optimum value of $\alpha_{profile}$ depends on the relative value of the refractive index increment, wavelength, and dispersion of the medium [16]:

$$\alpha_{profile,optimal} = 2 - 2P - \Delta_{rel}\frac{(4-2P)(3-P)}{(5-4P)}, \qquad (3)$$

where P is the dispersion parameter of the profile

$$P = \frac{n_1}{n_1 - \frac{dn_1}{d\lambda}} \times \frac{\lambda}{\Delta_{rel}} \times \frac{d(\Delta_{rel})}{d\lambda} \qquad (4)$$

In the range of small concentrations of the impurities phosphorus pentoxide, $\alpha_{profile} \approx 2$ [16].

Manufacturing of the fiber preforms

For implementation of the highly transparent and broadband in the UV range fibers, we have chosen two types of graded profiles of the refractive index: the "depressive" with respect to refractive index of silica glass and the "highly refracting".

The "depressive" RIP was realized using the fluoride doping, while the "highly-refractive" RIP was achieved by adding phosphorus pentoxide. The absolute value of the refractive index increment was about 0.0050, which provided the nominal aperture 0.12 – 0.13 at the wavelength 350 nm. This low value of the aperture was chosen for reasons of minimization of the losses and radiative sensitivity of the fiber. Note that heavy doping of the glasses with phosphorus leads to additional technological problems, namely, to a strong decrease in the deposition rate, increased expenses of raw materials, etc. For the fluorine-containing glasses, the fibers with larger apertures may be manufactured.

The preforms were made using the MCVD technique, with the tubes "Heralux" of "Heraus" company used as the bearings.

The fluorine doping was implemented using different reagents: silicon tetrafluoride, carbon tetrafluoride, freons $C_2Cl_3F_3$ and CCl_2F_2, whose use was demonstrated previously in [17–19].

At a strong excess of the fluorinating component, no deposition of silica occurs; instead the process of its etching goes according to the reaction

$$3[SiO_{4/2}]+SiF_4+2Cl_2 \rightarrow 4SiF_3Cl\uparrow+O_2\uparrow$$

For the reaction of fluorination of the glass,

$$3[SiO_{4/2}]+ SiF_4 \rightarrow 4[SiO_{3/2}F]$$

the partial pressure of $[SiF_4]$ and, hence, its concentration should be much lower. The process goes in proper direction at small values of partial pressure of $[SiF_4]$, and the refractive index changes due to decreasing fluorine concentration from the periphery of the core toward its center. The fluorine concentration in the glass is proportional to partial pressure of the tetrafluoride to the 1/4 power [19]. A characteristic feature of these preform is the absence of a dip in the vicinity of r=0.

To increase the efficiency of the process, we used, as the starting reagent, sulfur hexafluoride SF_6.

We have manufactured preforms with the RIP close to that shown in Figure 1a. From these preforms, we have drawn a fiber whose spectrum is shown in Figure

2. As is seen, the fiber shows an intense band at $\lambda = 330$ nm, which indicates a high content of chlorine in the fiber ($\alpha_{330\ nm} \approx 900$ dB/km).

In the process of working out of the preform technology, we have found that at low consumption of sulfur hexafluoride (Q_{SF6}) the dependence $|\Delta n_F| = f(Q_{SF6})$ is much more steeper than it follows from [19], which points to different refraction of fluorine in the range of low and moderate concentrations. This is likely to be related to the fact that the fluorine atoms are initially localized at defect sites of the network and then, with increasing concentration, they change the sites of their localization.

To reduce concentration of the dissolved chlorine (the band at 330 nm), the preforms were specially treated. This was accompanied by a strong decrease of absorption in the spectral range under study (Figure 2).

The level of losses reliably achieved at the wavelength 350 nm was 100 – 120 dB/km, which was considered as a very good result. Recall that the limiting losses for scattering, in this spectral region, lie in the range of 80 – 90 dB/km.

It should be noted, however, that the process of manufacturing of the fluorine-containing glasses was rather labor-consuming and low-efficient. This is why we turned to the "highly refractive" profile of the refractive index.

The "highly refracting" RIP was obtained by doping the silica with quinquivalent phosphorus, introduced using the phosphorus oxychloride ($POCl_3$) (i.e., adding phosphorus pentoxide) at the stage of manufacturing preform. Figure 1b shows the relevant RIP in the preform. The profile is characterized by a dip in the refractive index, which is formed because of reduction of the phosphorus concentration in the central zone of the core. The absorption spectrum of the fiber is shown in Figure 3. Note that although the average level of losses at λ=350 nm, for the phosphate fibers, lies in the range of 120 – 150 dB/km, which was substantially worse than for fluoride-containing fibers, the low losses were achieved with no special treatment of the preforms. The efficiency of the deposition process was fairly satisfactory, with a sufficiently high productivity.

We have performed studies aimed at optimization of the ratio of the core and fiber diameters. It is shown that the losses slightly decreased with increasing diameter of the core.

For the signal transmission, we supposed to manufacture 19-core cables in the standard 125/100. The further measurements of the losses and pulse broadening, however, have shown that the fibers in bundles exhibit lower relative transmittance because of low filling factor and additional broadening of the pulse. For this reason, we made an attempt to replace the bundles by a large-diameter monofiber with the diameter of the outer cladding 600 μm and diameter of the core 435 μm. The level of the losses achieved at the wavelength 350 nm lay between 120 – 150 dB/km.

The pieces of the fibers used in the framework of the NIF LLNL program were 1.2, 6.0, 10.0, 20.0, 24, 27, and 30.0 m in length. The transmittance of these pieces was tested before installation. Figure 4 shows dependence of transmittance of the elements with different length versus the length. This figure confirms that the predominant part of the fiber may be characterized by the losses at the wavelength 350 nm lying in the range of 120 – 150 dB/km.

A similar dependence of the dispersion per meter run (δ, psec/m) is shown in Figure 5 for the fiber cables of different length. The parameter of the dispersion per unit length was determined by measuring broadening of ultrashort laser pulses upon their propagation through the fiber line. Under assumption of Gaussian shape of the initial pulses, the relation between the initial pulsewidth (τ_0), instrumental time resolution of the fiber line (Δ), and the pulsewidth at the exit of the fiber system (τ_{fiber}) is given by the expression

$$\tau_{fiber}^2 = \tau_0^2 + \Delta^2 \qquad (5)$$

The instrumental time resolution Δ specifies the time dispersion of the particular cable.

The fiber cables are usually characterized by the time dispersion per unit length $\delta = \frac{\Delta}{L}$, where L is the length of the fiber line. Note once again that the parameter δ is not the dispersion parameter of the fiber, but it rather specifies the dispersion characteristics of the particular fiber cable, because the parameter δ is not additive in length.

The fiber proper may be characterized by the time dispersion parameter β, determined from the additivity conditions for the instrumental dispersion function of the fiber line. Assuming that Δ_i is the dispersion characteristic of a cable with a unit length, for the cable comprised of the segments of unit length, this expression acquires the form

$$\tau_{fiber}^2 = \tau_0^2 + \sum_{i=1}^{N} \Delta_i^{\,2}, \qquad (6)$$

and the time dispersion parameter β is determined by the expression

$$\beta = \frac{\Delta^2}{L} = \delta^2 \times L \qquad (7)$$

Now, for the above method of finding the pulse broadening, the parameter β does not depend on the length of the sample tested (unlike the dispersion per unit length δ).

It follows from the aforesaid that the dispersion per unit length decreases in magnitude with increasing length of the fiber cable, which is confirmed experimentally.

The time dispersion of the fiber was determined experimentally by comparing the width of the pulse transmitted by the fiber sample with the width of a reference pulse transmitted by an air delay line of the relevant length. For testing, we used single pulses with a pulses width of about 20 psec in the vicinity of λ = 342 nm with the energy E ~10^{-9} J. Figure 6 shows chronograms of the pulses at the entrance and at the exit of 25-m cable and 40-m sample of the fiber. Here, the value of the dispersion per unit length for the 40-m sample (δ = 0.52 psec/m) corresponds to the time dispersion parameter β = 9.5 psec^2/m, while in the 25-m sample drawn from the same preform (β = 9.6 psec^2/m) (difference between values 9.5 psec^2/m and 9.6 psec^2/m is within the precision of measurements), the dispersion per unit length increases to δ = 0.62 psec/m.

Conclusions:

1. Two types of fibers for distortion-free transmission of subnanosecond UV optical pulses are developed.

2. A technology for manufacturing preforms and drawing large-diameter monofibers is developed, providing losses below 150 dB/km and pulse broadening smaller than 0.9 psec/m at the wavelength 351 nm.

3. The large-diameter monofibers make it possible to transmit nanosecond-range signals with very small distortions and to do away with the concept of the bundles system for achieving large apertures.

4. The fiber elements for the National Ignition Facility, meeting all the specifications, are manufactured and delivered to the LLNL.

References

[1] NIF Laser System Performance Rating, Supplement to Proceedings of SPIE, 1998, vol. 3492.

[2] Sorokin, Yu.M. and Shiryaev, V.S., Optical losses in optical fibers, 2000, Nizhni Novgorod, 19-22.

[3] Khalilov, V.Kh., Fiz. Khim. Stekla, 1983, 9, no. 2, 145-147.

[4] Gurnovskii, E.V., Khalilov V.Kh., and Leko, V.K., Physico-chemical studies of structure and properties of silica glass, 1974, 1, 45-52

[5] Khalilov, V., Guskov, M.I., Dorfman, G., Danilov, E., and Ermakov, V., 1993, ISFOC, 239-242.

[6] Khalilov, V., Dorfman, G., Danilov, E., and Guskov, M.I., J.Non-Gryst.Solids, 1994, 169, 15-28.

[7] Silin', A.R. and Trukhin, A.N., Point defects and elementary excitations in the crystalline and vitreous SiO_2, 1985, Riga, Zinatne, 15-28.

[8] Keck, D.B., Maurer, R.D., and Shultz, P.C., 1973, Appl.Phys.Lett., 22, 307-313.

[9] Amosov, A.V., Khalilov, V.K., and Pivovarov, S.S., 1981, Fiz. Khim. Stekla, 7, no. 3, 336-338.

[10] Greaves, G.N., J.Non-Cryst. Solid, 1979, 32, 295-297.

[11] Abramov, A.D., Anokhin, E.V., Dianov, E.M., Highclean Substance (USSR), 1987, 12.

[12] Hanafusa, H., Hibino, Y., Yamamoto, F., J. Appl. Phis., 1985, 58, 3, 1356-1361.

[13] Hibino, Y, Hanafusa, H., J.Appl. Phys., 1986, 60, 5, 1797-1801.

[14] Pinnov, D.A., Rich, T. C., Ostermayer, F.W., and Di Domerico, M., 1973, J.Appl Phys. Lett.

[15] Eve, M., Electron. Lett., 1977, 13, 315-320.

[16] Sladen, F.M.E., Payne, R.N., and Adams, M.J., Proc. 4th ECOC, 1978, 48-57.

[17] Abe, E, 2nd Europen conf. on optical communication.

[18] Bogdanova, O.Yu., Eron'yan, M.A., Zhakhov, V.V., and Berezhkov, V.B., Proceedings of All-Union Conference on Technology of Optical Fibers, 1982, Gor'kii, 51-52.

[19] Valker, K.Z., et al., 6th Topical Meet. Opt. Fiber Commun., 1983, New Orlean, 34-41.

a)

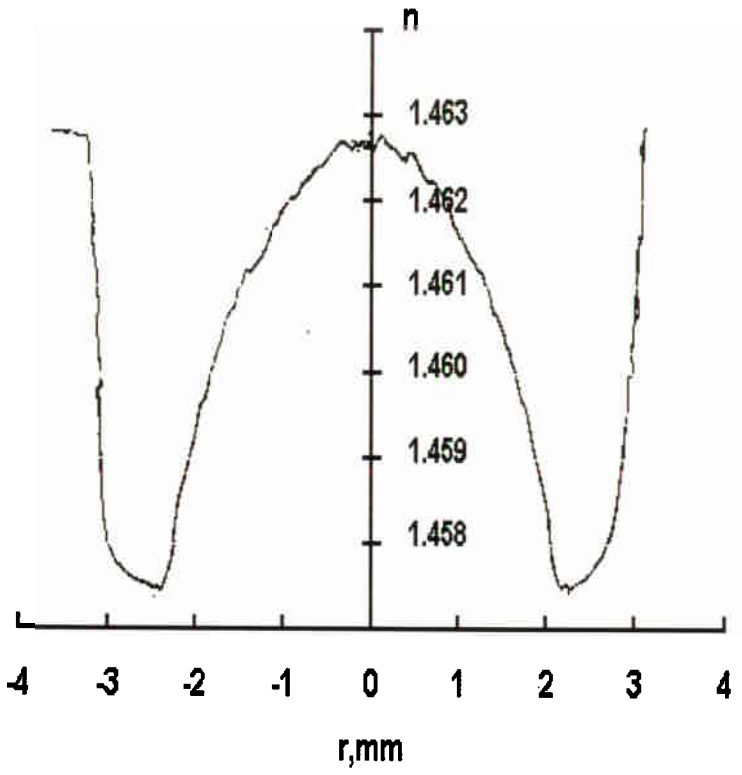

b)

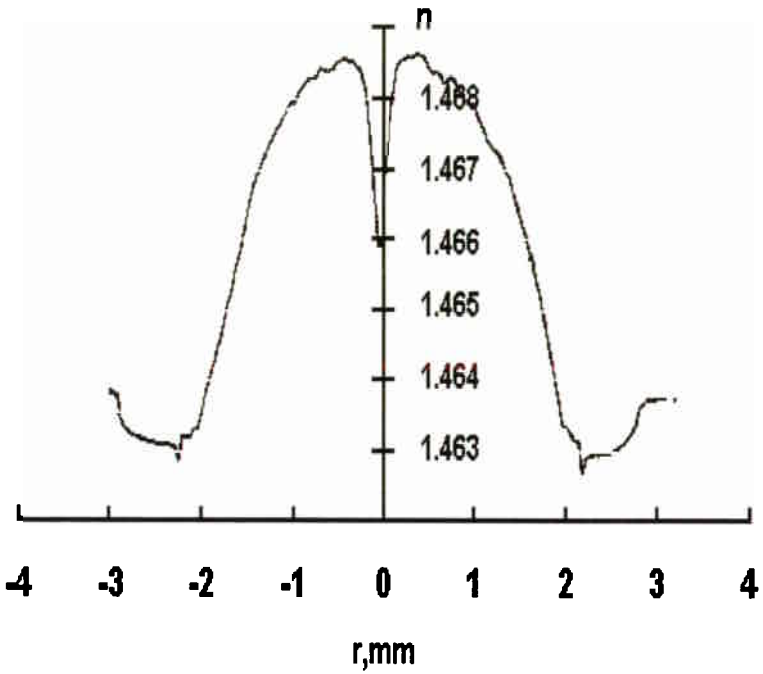

Figure 1. Refractive index profiles of the preforms:
a) "depressive" (SiO_2+F)
b) "highly refracting" (SiO_2+P_2O_5)

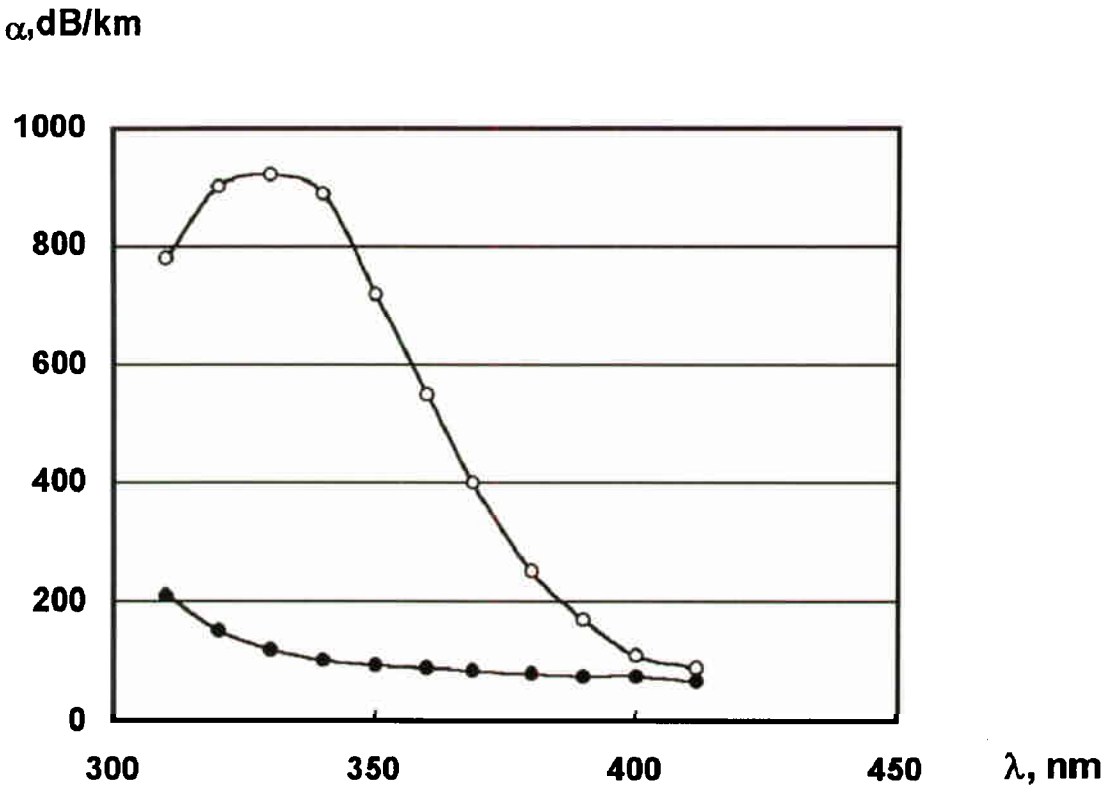

Figure 2. Spectral behavior of losses of the fiber (SiO_2+F)
in the near UV range.
"white circles" – before the special treatment,
"black circles" – after the special treatment.

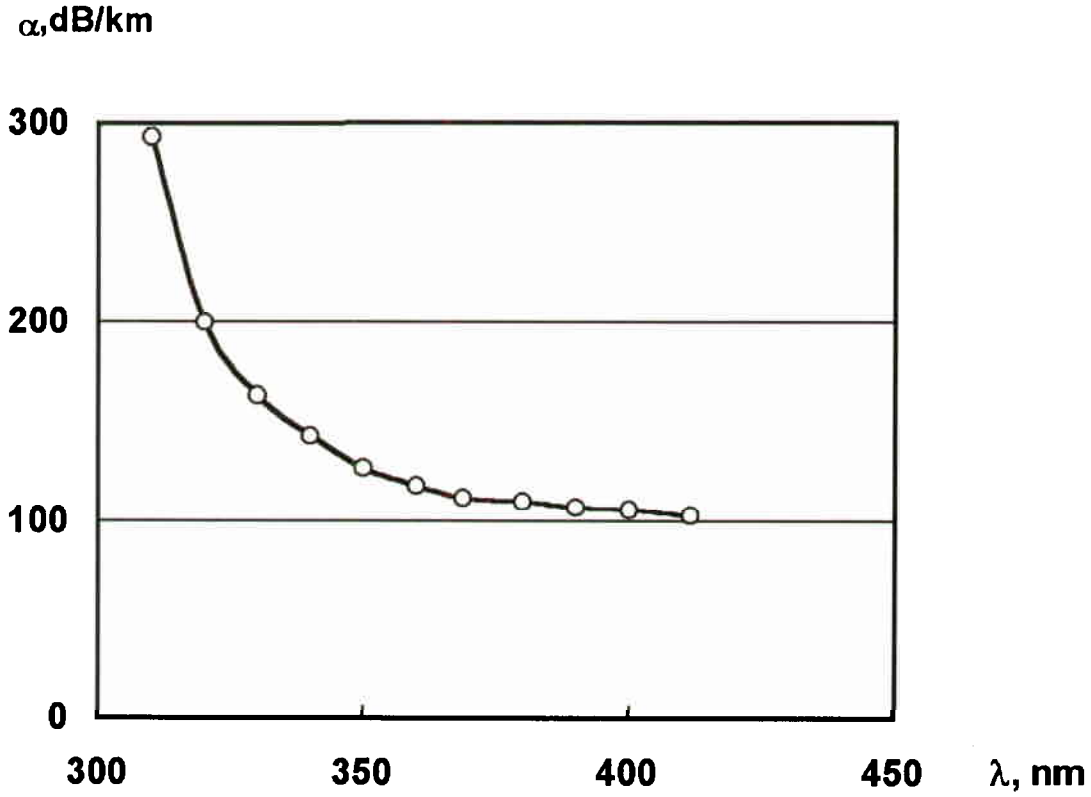

Figure 3. Spectrum of the fibers with the "highly refracting" profile (SiO_2+P_2O_5) without special treatment.

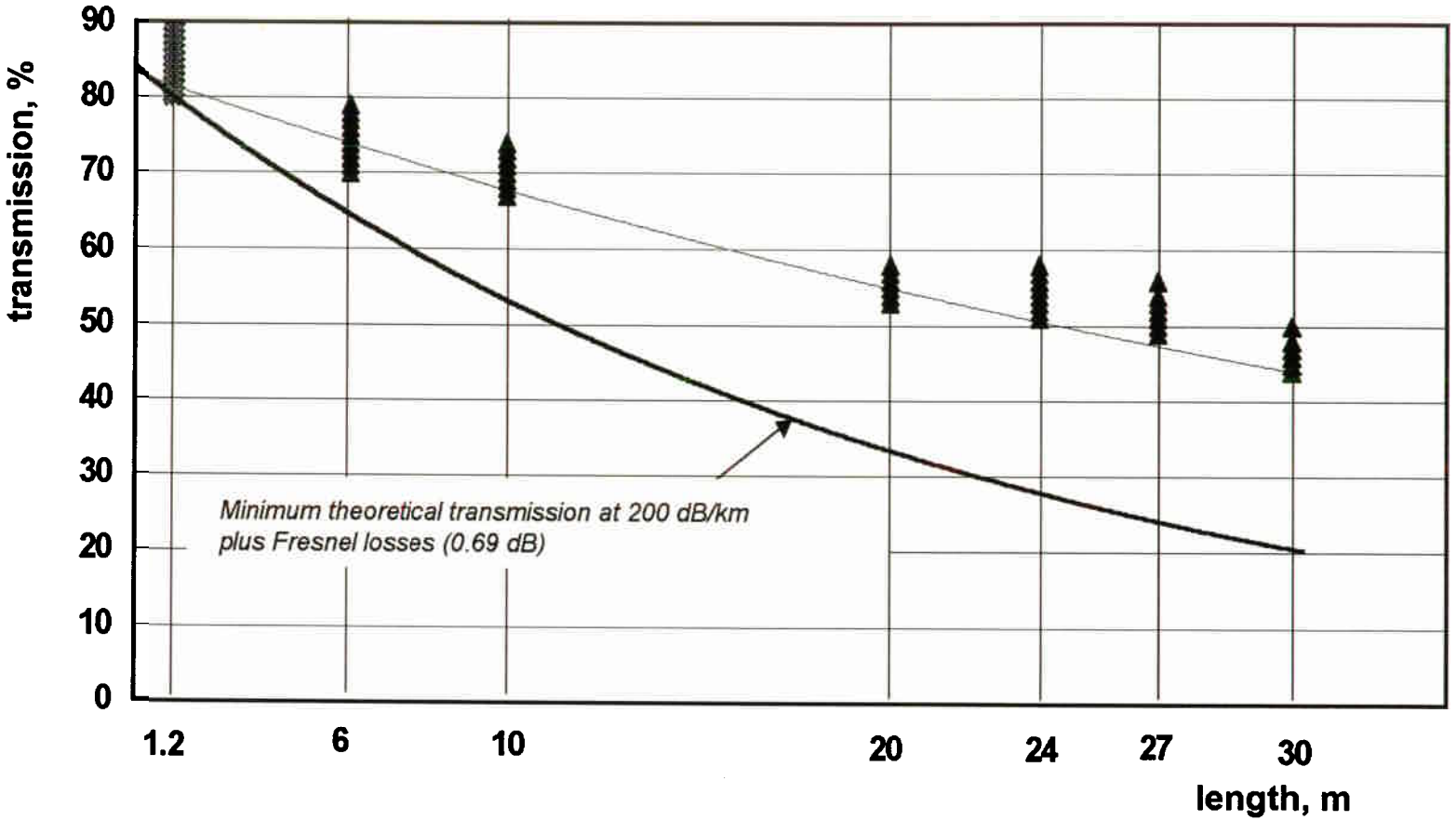

Figure 4. Light transmission of the "highly refracting" fiber-optic cables (including Fresnel losses) based on the UV fiber as a function of the length. The attenuation of the fiber is ~ 100 dB/km (0.1 dB/m).

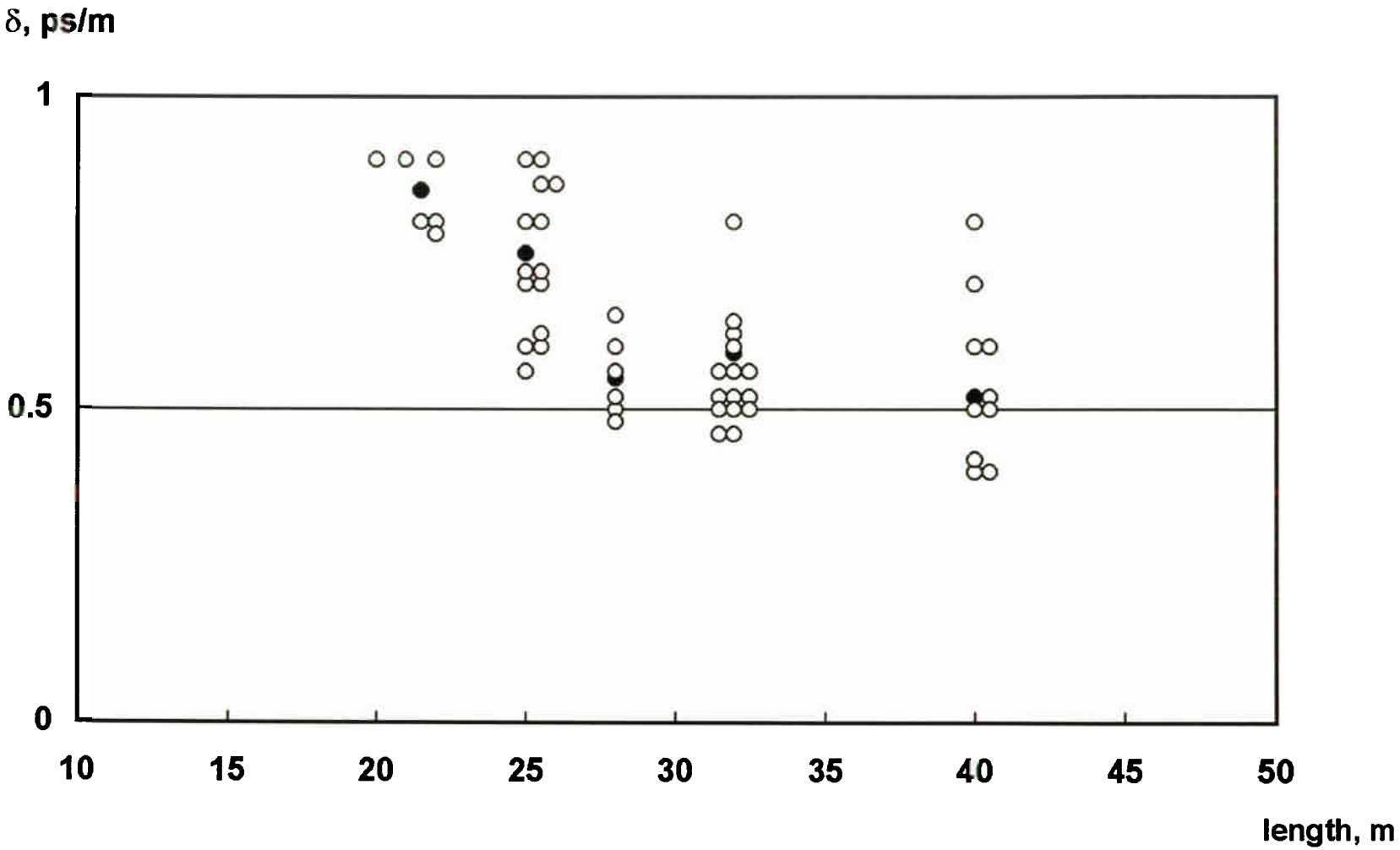

Figure 5. Dependence of the broadening per unit length on the cable ("highly refracting") length ("black circles" – averaged values). The 40-m long samples are fiber parts.

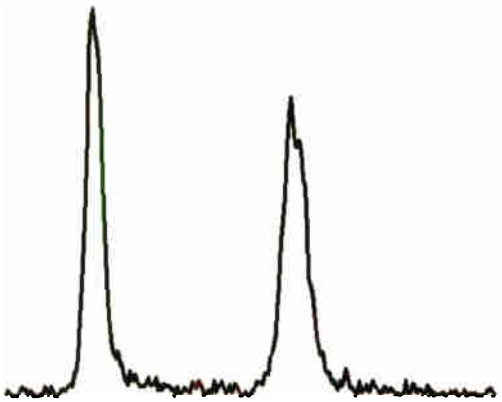

$\delta = 0.62$ psec/m
$\beta = 9.6$ psec^2/m
L=25 m

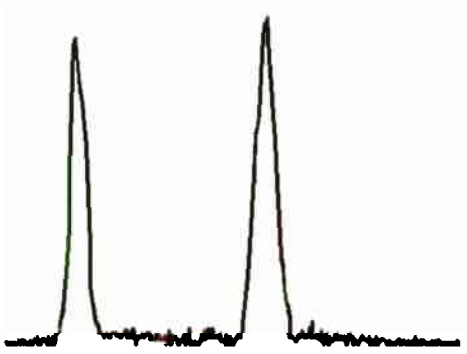

$\delta = 0.52$ psec/m
$\beta = 9.5$ psec^2/m
L=40 m

Figure 6. Real pulse shapes for the cable 25-m and fiber 40-m long manufactured from "highly refracting" fibers of the same preform (difference between values 9.5 psec^2/m and 9.6 psec^2/m is within the precision of measurements).